https://doi.org/10.5194/egusphere-2026-3909
Preprint. Discussion started: 24 July 2026

Assessing the Representativeness of Surface Atmospheric Ammonia Observations for Satellite Data Interpretation

Camille Viatte[1], Vincent Lécluse[2], Antoine Causse[3], Marion Delidais[4], Mélodie Chatain[2], Mathilde Bourlon[3], Ángel Luque Lázaro[1,5], Jérôme Le Paih[2], Julie Cozic[3], and Guillaume Salque-Moreton[3].

[1] LATMOS/IPSL, Sorbonne Université, UVSQ, CNRS, Paris, France ;

[2] ATMO Grand Est, 5 rue de Madrid, 67300 Schiltigheim, France ;

[3] Atmo Auvergne Rhône-Alpes, 3 Allée des Sorbiers, 69500 Bron, France ;

[4] AirBreizh, 3E rue de Paris, 35110 Cesson-Sévigné, France ;

[5] SPASCIA, Ramonville-Saint-Agne, Toulouse, France ;

Correspondence to: Camille Viatte (Camille.viatte@latmos.ipsl.fr)

https://doi.org/10.5194/egusphere-2026-3909
Preprint. Discussion started: 24 July 2026

Abstract. Atmospheric ammonia (NH_3) is a major precursor of secondary fine particulate matter and is predominantly emitted by agricultural activities. However, the representativeness and complementarity of satellite and surface NH_3 observations remain insufficiently characterized. This study evaluates the consistency between IASI satellite observations and surface NH_3 measurements across the three largest NH_3 emitting regions of France (Brittany, Grand Est, and Auvergne–Rhône-Alpes), representing 44% of national emissions. A network of 24 monitoring sites, equipped with Radiello passive samplers and Picarro analyzers, operates from June 2024 to June 2025. Surface measurements show higher and more variable NH_3 concentrations at agricultural sites than at background sites, whereas traffic-influenced urban locations exhibit intermediate levels. IASI NH_3 columns reproduce surface regional patterns and seasonal variability, with spring and summer maxima consistent with agricultural emissions. Satellite–surface agreement is assessed across multiple spatial and temporal scales. Strong correlations ($R \geq 0.7$) are obtained at biweekly to seasonal timescales when averaging IASI observations within 20–40 km of the monitoring sites, demonstrating its capability to characterize regional NH_3 variability. In contrast, correlations remain weaker at daily and sub-daily timescales, highlighting the limited ability of polar-orbiting satellites to capture localized variability. These findings demonstrate that satellite observations are well suited for long-term NH_3 monitoring and trend analysis, whereas dense surface networks remain essential for resolving fine-scale variability. The forthcoming IRS geostationary mission should improve NH_3 monitoring through enhanced temporal and spatial sampling.

https://doi.org/10.5194/egusphere-2026-3909
Preprint. Discussion started: 24 July 2026

Cover Letter. Ammonia (NH_3) is an important air pollutant mainly emitted by agricultural activities such as livestock farming and fertilizer application. Once released into the atmosphere, NH_3 contributes to the formation of fine particulate matter, which affects human health, ecosystems, and climate. Monitoring NH_3 concentrations is therefore essential for improving air quality and supporting emission reduction policies. Satellite instruments such as IASI (Infrared Atmospheric Sounding Interferometer) provide large-scale and near-daily observations of atmospheric NH_3, while ground-based measurements offer more precise information at the local scale. However, the complementarity between these two types of observations remains insufficiently understood.

In this study, satellite and surface NH_3 measurements were compared across the three largest emitting regions of France: Brittany, Grand Est, and Auvergne–Rhône-Alpes. A network of 24 surface monitoring sites was deployed between June 2024 and June 2025 to investigate how local emission sources and meteorological conditions influence NH_3 variability. Agricultural sites generally showed higher and more variable concentrations than background sites, while urban traffic-influenced locations exhibited intermediate levels.

The results show that satellite and surface observations are consistent at regional and multi-day timescales, especially when observations are averaged over periods of about two weeks and spatial scales of 20–40 km. This demonstrates that satellite observations are well suited for long-term monitoring of NH_3 surface variability and trends. In contrast, weaker agreement was found at daily and local scales, where surface measurements remain essential to capture rapid changes and localized emission sources such as traffic or nearby agricultural activities.

Overall, the study highlights the strong complementarity between satellite and ground-based observations for atmospheric NH_3 monitoring. While satellites provide valuable regional coverage, surface measurements remain necessary to validate satellite products and better characterize local-scale processes. Future satellite missions with improved spatial and temporal resolution are expected to further strengthen these monitoring capabilities.

https://doi.org/10.5194/egusphere-2026-3909
Preprint. Discussion started: 24 July 2026

1 Introduction

Atmospheric ammonia (NH_3) is a major precursor of secondary fine particulate matter through the formation of ammonium salts [Sutton et al., 2013], which are very harmful to public health [Pope III et al., 2009]. Global NH_3 emissions increased by more than 80% between 1970 and 2017 [McDuffie et al., 2020] with agricultural activities accounting for more than 93 % of emissions in Europe [European Environment Agency, 2020]. To comply with the National Emission reduction Commitments Directive (NEC) Directive, Europe must reduce its emissions by 13% by 2030 (relative to 2005 levels). Mitigating atmospheric NH_3 emissions remains difficult because they are closely tied to agricultural productivity and food security under continued global population growth [Aneja et al., 2020]. Sustained increases in livestock production and fertilizer application required to support food demand limit the potential for large emission reductions without impacts on crop yields [Beaudor et al., 2025]. Moreover, increasing temperatures are expected to enhance NH_3 volatilization from soils and manure, potentially further increasing atmospheric NH_3 concentrations [Liu S. et al., 2024]. Finally, its potential uses as fuel options for transportation [Azim et al., 2024] should further increase its emissions. NH_3 emission regulation remains limited compared to other pollutant, such as sulfur dioxide (SO_2) and nitrogen oxides (NOx) [Sutton et al., 2013].

Current evaluations of atmospheric NH_3 emission changes are not straightforward and rely on estimations based on bottom-up or top-down approaches involving various atmospheric variables (emission factors, meteorological fields, pollutant concentrations). The lack of surface ammonia measurements limits the ability to evaluate mitigation policies to reduce emissions. The revised European Directive 2024/2881 now makes NH_3 concentration measurements mandatory in Europe in rural environments and recommended in urban areas [European Environment Agency, 2024]. However, there is still no reference method for sampling and measuring NH_3 concentrations. Ammonia observations are very challenging from a sampling and metrological point of view: it is a polar, sticky, reactive and highly water-soluble molecule, resulting in strong interactions with sampling systems [da Silva et al., 2023; Twigg et al., 2022; Ellis et al., 2010; Von Bobrutzki et al., 2010]. In addition, NH_3 concentrations are highly variable spatially and temporally which is due to the spatial heterogeneity of sources and its relatively short lifetime in the atmosphere which is estimated to range from a couple of hours to a couple of days [Xie et al., 2024; Evangeliou et al., 2021; Dammers et al., 2019]. Few countries routinely measure NH_3 worldwide, using low-cost, low time resolution methods deployed on a large number of sites [Ma et al., 2025; Nair and Yu, 2020].

In Europe, the oldest network was developed in the United Kingdom [Tang et al., 2018; Sutton et al., 2001] and in the Netherlands [Berkhout et al., 2017; Lolkema et al., 2015; Buijsman et al., 1998] in the 1990s to address spatial patterns of NH_3 concentrations with low frequency sampling (every week to monthly) using the Denuder for Long Term Atmospheric (DELTA® sampler [Sutton et al., 2001] and the Adapted Low-cost, Passive High Absorption (ALPHA® diffusive samplers [Tang et al., 2001]. These relatively low-cost instruments are chosen for their long-term stability and accuracy. Radiello instruments are also common low frequency sampling instruments used to monitor NH_3 concentrations [Zhu et al., 2015] with a quantified low bias (37%) compared to the referenced method by denuders [Puchalski et al., 2011]. The availability of these long-term datasets has improved the understanding of atmospheric NH_3 behavior, particularly through the quantification of

https://doi.org/10.5194/egusphere-2026-3909
Preprint. Discussion started: 24 July 2026

wet and dry deposition processes [Zanten et al., 2017; Bleeker et al., 2009], the gas-particle interconversion [Cheng et al., 2021; Tang et al. 2009; Singh et al., 2001] and give further insights to develop effective $PM_{2.5}$ control strategies [Sutton et al., 2003]. Later, high frequency measurements (every minute) of NH_3 concentrations, needed to study its atmospheric processes (source and sink), were also implemented in the Netherlands using mini-DOAS instruments [Volten et al., 2012]. High-frequency (minute or hour) measurements are very rarely used in these operational networks (with the notable exception of the Netherlands, with a small number of open-path mini-DOAS 'supersites'), precisely because of the great difficulty of sampling NH_3 without bias (memory effect, [Kim et al., 2021]) and also the difficulty of properly calibrating spectroscopic analyzers in the low concentration ranges (< a few ppb) encountered in certain remote areas.

With the inclusion of NH_3 concentrations monitoring in both rural and urban environments stated in the revised directive, the number of NH_3 observations will rapidly grow across Europe. A recent study that analyses variability of NH_3 concentrations across 69 monitoring sites in five European countries (Finland, France, Italy, Spain, and the UK), emphasizes that the use of many different measurement protocols could have a negative impact on the comparisons [Liu X. et al., 2024]. Harmonization of NH_3 measurements protocols and data processing is critical to implement the future homogenous and efficient ammonia networks in Europe.

To prevent from the lack of surface measurements, many recent studies have used NH_3 satellite observations in combination with an atmospheric chemical transport models to estimate global [Luo et al., 2022; Van Damme et al., 2021; Cao et al., 2020], regional [Ding et al., 2024; Tichy et al., 2023] or even local NH_3 [Marais et al., 2021; Van Damme et al., 2018] emissions. Satellite observations of NH_3 concentrations provide global, near-daily coverage, including the Infrared Atmospheric Sounding Interferometer (IASI, [Clerbaux et al., 2009]), the Atmospheric Infrared Sounder (AIRS, [Warner et al., 2016]), the Cross-track Infrared Sounder (CrIS, [Shephard & Cady-Pereira, 2015]) and the Tropospheric Emission Spectrometer (TES, [Shephard et al., 2011]), all operating in the thermal infrared spectral range.

While satellite observations offer near-daily global observations of NH_3 total columns, ground-based measurements offer precise, localized information on surface NH_3 concentrations and variabilities. Multiple factors complicate the integration of surface network and satellite measurements due to their substantially different spatiotemporal scales [Wang et al., 2023]. Spatio-temporal criteria strongly affect the comparison results. Satellite observations are commonly validated against ground-based Fourier-transform InfraRed spectroscopy (FTIR) observations, both providing vertically integrated NH_3 column concentrations. IASI NH_3 total column retrievals have been validated against FTIR observations at multiple sites worldwide, generally showing moderate to strong correlations ($R \sim 0.47–0.83$) using coincidence criteria of ~25 km and <90 min [Wang et al., 2022; Yamanouchi et al., 2021; Dammers et al., 2016]. Similar agreement was reported for CrIS retrievals, although with larger inter-site variability ($R \sim 0.28–0.84$) [Dammers et al., 2017]. However, FTIR observations still lack extensive validation against independent in situ measurements.

Only a limited number of studies have evaluated the consistency between satellite NH_3 columns and surface measurements. Moderate to strong correlations have been reported between monthly surface NH_3 concentrations and CrIS columns in China ($R = 0.79$) [Sun et al., 2025], between biweekly passive sampling and IASI observations in the United States ($R = 0.74$) [Wang

https://doi.org/10.5194/egusphere-2026-3909
Preprint. Discussion started: 24 July 2026

et al., 2023], and between IASI and ground-based miniDOAS measurements in central Paris over 2.5 years (R = 0.69) [Viatte et al., 2023]. Very few studies have examined the consistency at the pixel scale, and those available have been largely restricted to high-emission source regions. TES NH_3 data were strongly correlated (R = 0.82) with surface measurements (±1.5 h of the TES overpass) over one of the largest NH_3 hot spots of United States (San Joaquin Valley) using nine TES pixels [Sun et al., 2015]. IASI data showed good agreement (R = 0.58) with *in situ* derived columns using a 15 km window around centroid, and a ±1 h window around the overpass time [Guo et al., 2021].

Despite their limited number, validation and intercomparison studies between ground-based measurements and satellite retrievals of NH_3 concentrations highlight the need for more in-depth analysis to better exploit both datasets. In this context, the ROSAS project ("Représentativité des Observations de Surface d'Ammoniac atmosphérique en appui à l'exploitation des données Satellites", funded by The French Agency for Ecological Transition ADEME) aims at assessing representativeness of surface measurements in support of satellite observations that require analyzing correlation coefficients while accounting for spatial and temporal variabilities. The objective is to determine the spatiotemporal scales at which IASI observations can reliably complement or substitute surface measurements, and under which conditions ground-based observations remain necessary to provide a comprehensive view of atmospheric NH_3 variability. This study targets the Brittany, Grand Est, and Auvergne–Rhône-Alpes regions, which collectively represent about 44% of total French NH_3 emissions. Agricultural activities dominate regional emissions, accounting for 91% in Grand Est and more than 99% in Brittany, primarily through livestock farming and fertilizer application. Exploiting the complementarity between satellite and ground-based measurements is needed for air quality and emission reduction policy-making. This study further extends validation efforts to enhance confidence in integrating these two datasets to explore a more comprehensive analysis of atmospheric NH_3.

2 Methodology

2.1 Ground-based NH_3 measurement sites during the ROSAS campaign

This study aims to quantify the spatial representativeness of NH_3 analyzers over an annual period across environments characterized by contrasting emission regimes, including cropland-dominated rural areas, livestock-intensive regions, and urban settings. Determining these representativeness scales is essential for interpreting ground-based measurements and for improving comparisons and validation efforts between IASI satellite observations and in situ NH_3 measurements. Given that the minimum IASI footprint corresponds to a circular area of about 12 km in diameter (~6 km radius), the spatial representativeness of surface analyzers within this domain must be evaluated. Therefore, a passive tubes campaign is deployed around three analyzers, one in each studied region (Figure 1). The passive tube locations and the campaign setup follow a common strategy detailed below:

- One year of measurements was conducted following a common sampling calendar to capture the annual periodicity of ammonia, with 2-week exposure periods except in spring when they were reduced to 1 week due to enhanced ammonia concentrations associated with agricultural activities.

https://doi.org/10.5194/egusphere-2026-3909
Preprint. Discussion started: 24 July 2026

- Seven tubes were deployed per sampling period: one at the analyzer location, two on a ~6km radius circle and four on a ~15km radius circle.
- Two transects of sampling points were defined by combining land use, emissions, and meteorological conditions (mainly wind), with four points along the most heterogeneous axis and two along the most homogeneous axis.
- Quality control was ensured through triplicates and blanks at the central analyzer location at least once a month.

Figure 1 illustrates the locations of tubes and the surrounding communal emission in each region.

For better homogeneity in the results, each region used PICARRO analyzers (SI2103) and Radiello passive tubes (R168). In terms of quality, the methodology of the Central Laboratory for Air Quality Monitoring (LCSQA) guide book (https://www.lcsqa.org/fr/rapport/guide-methodologique-pour-la-mesure-des-concentrations-en-ammoniac-dans-lair-ambiant) was applied for measurement and validation.

A minimum spatial window with a radius of 15 km was adopted, consistent with the characteristic spatial extent of NH_3 hotspots reported by Wang et al. (2021; 2023).

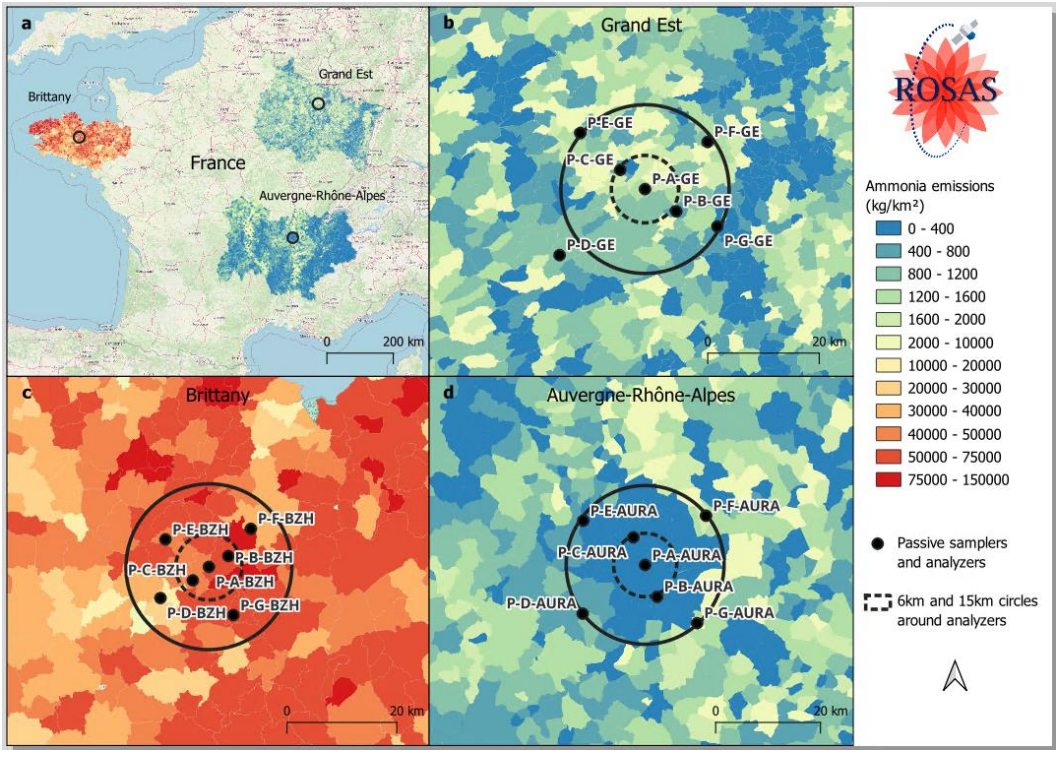

Figure 1: Schematic representation of the ROSAS project. Map of France with regions of interest color-coded by ammonia emissions (a). Locations of surface ammonia passive samplers during the ROSAS campaign (June 2024 – June 2025) in the Grand Est region (b). Same for Brittany (c) and Auvergne-Rhône-Alpes (d) regions.

https://doi.org/10.5194/egusphere-2026-3909
Preprint. Discussion started: 24 July 2026

Table 1: Summary of surface measurement sites and characteristics during the ROSAS campaign.

Region	Brittany							
Obs. type	passive sampler							analyzer
City	Kergoff	Merléac	Etang de Poulancre - Saint-Gilles-Vieux-Marché	Caurel	Le Haut-Corlay	Allineuc	Saint-Caradec	Kergoff
Latitude	-2.944	-2.896	-2.983	-3.062	-3.050	-2.842	-2.884	-2.944
Longitude	48.262	48.280	48.240	48.211	48.307	48.324	48.184	48.262
ID ROSAS	P-A-BZH	P-B-BZH	P-C-BZH	P-D-BZH	P-E-BZH	P-F-BZH	P-G-BZH	A-A-BZH
Incidence	Rural	Livestock	Livestock	Livestock	Livestock	Cropland	Livestock	Rural
Region	Grand Est							
Obs. type	passive sampler							analyzer
City	Jonville	Hagéville	Harville	Lamorville	Braquis	Doncourt-lès-Conflans	Villecey-sur-Mad	Jonville
Latitude	49.066	49.030	49.097	48.960	49.156	49.141	49.006	49.066
Longitude	5.786	5.862	5.725	5.577	5.628	5.938	5.962	5.786
ID ROSAS	P-A-GE	P-B-GE	P-C-GE	P-D-GE	P-E-GE	P-F-GE	P-G-GE	A-A-GE
Incidence	Livestock	Livestock	Livestock	Livestock	Livestock	Livestock	Cropland	Livestock
Region	Auvergne-Rhône-Alpes							
Obs. type	passive sampler							analyzer
City	Lyon	Vénissieux	Saint-Cyr au mont d'or	Soucieu	Dommartin	Beynost	Toussieu	Lyon
Latitude	4.854	4.884	4.826	4.702	4.703	5.003	4.981	4.854
Longitude	45.758	45.704	45.805	45.675	45.833	45.842	45.659	45.758
ID ROSAS	P-A-AURA	P-B-AURA	P-C-AURA	P-D-AURA	P-E-AURA	P-F-AURA	P-G-AURA	A-A-AURA
Incidence	Traffic	Background	Background	Background	Background	Background	Background	Traffic

2.2 IASI NH_3 dataset

Atmospheric NH_3 total columns are obtained from the Infrared Atmospheric Sounding Interferometer (IASI) measurements [Clerbaux et al., 2009], a Fourier Transform Spectrometer (FTS) flying onboard the Metop-A, Metop-B and Metop-C satellites in a Sun-synchronous polar orbit (approx. 817 km altitude). IASI measures the thermal infrared radiation emitted by the Earth and the atmosphere in the 645 to 2760 cm^{-1} spectral range with a spectral resolution of 0.5 cm^{-1} (after apodization). The

https://doi.org/10.5194/egusphere-2026-3909
Preprint. Discussion started: 24 July 2026

instrument has a wide swath of approximately 2200 km, providing near-global coverage twice daily with overpass times at approximately 09:30 and 21:30 local solar time. At each sampling point, IASI observes a 2x2 matrix of four circular pixels, each with a diameter of 12 km at nadir. For this study, we use the reanalyzed Level 2 (L2) ammonia product retrieved using the Artificial Neural Network for IASI (ANNI) version 4 (v4) algorithm [Clarisse et al., 2023]. This version converts a hyperspectral range index (HRI) into total column abundances (in molecules.cm^{-2}) using a feed-forward neural network and provides associated averaging kernels to account for the vertical sensitivity of the retrieval. In this study, a 20% cloud fraction cover is used for the IASI data selection.

2.3 Emissions and station incidence estimates

Potential NH_3 emission sources surrounding each monitoring site are characterized using a combination of agricultural land-use data, livestock distribution, and field observations. A detailed description of the potential NH_3 emission sources surrounding each monitoring site is provided in supplemental information S1. Agricultural land use is obtained from the 2024 Graphical Parcel Register (RPG) provided by the French National Institute of Geographic and Forest Information (IGN; https://artificialisation.developpement-durable.gouv.fr/bases-donnees/registre-parcellaire-graphique), while livestock information is derived from the Annual Agricultural Statistics (SAA) (https://agreste.agriculture.gouv.fr/agreste-web/methodon/S-SAA/methodon/) and distributed through the national PRISME platform (https://www.atmo-france.org/actualite/prisme-la-plateforme-air-climat-energie-pour-la-transition-ecologique).

For each monitoring station, circular buffers with radii of 500 m and 1 km are generated to characterize the surrounding environment potentially influencing the measurements. Within these buffers, RPG parcels are extracted, grouped into homogeneous crop categories (e.g., winter wheat, permanent grassland, grain maize), and their relative surface coverage is calculated. Livestock numbers are converted into Livestock Units (LU) to harmonize animal species before being spatially allocated to each monitoring site according to municipal boundaries.

The land-use and livestock datasets are combined with site visits and local expert knowledge to classify each station according to (i) its site typology (background, rural, traffic-influenced, etc.) and (ii) its dominant emission influence (livestock farming, crop cultivation, road traffic, or regional background). Agricultural sites are identified by the predominance of agricultural land (>70% within the surrounding buffer), together with crop composition and livestock density, whereas traffic-influenced sites are defined by their proximity to major roads. Regional background sites are selected to minimize the influence of local anthropogenic sources.

The selection and classification of rural sites follow the recommendations of the French MERA network (https://www.lcsqa.org/fr/le-dispositif-mera) and the European EMEP monitoring program (https://unece.org/fileadmin/DAM/ie/capact/ppp/pdfs/rws2/emep_man_e.pdf), ensuring regional representativeness while limiting the influence of nearby point sources. This methodology provides a consistent framework for interpreting NH_3 observations, comparing monitoring sites, and assessing the representativeness of the monitoring network with respect to the dominant emission sources across Brittany (Figure S1).

https://doi.org/10.5194/egusphere-2026-3909
Preprint. Discussion started: 24 July 2026

2.4 Meteorological parameters

As part of the ROSAS project, a cross-analysis between ground-based measurements (passive samplers and analyzers), satellite observations, and meteorological data is required. This comparison helps identify the influence of atmospheric conditions on NH_3 concentrations. Meteorological data is collected at the nearest stations of Météo France (https://donneespubliques.meteofrance.fr/).

The selected meteorological parameters are:

- Temperature (°C), influencing NH_3 volatilization.
- Wind direction, helping identify the origin of air masses transporting ammonia.
- Wind speed, affecting the dispersion of pollutants.
- Relative humidity (RH), playing a role in the transformation and persistence of NH_3 in the atmosphere.
- Precipitation, promoting the wet deposition of ammonia.

The objective is to use these data to improve the interpretation of NH_3 measurements and to better understand the processes of dispersion and concentration under local meteorological conditions.

2.5 Comparisons between IASI and surface NH_3 observations

To assess the added value of IASI NH_3 observations to surface monitoring networks, a detailed comparison with ground observations across various temporal and spatial scales has been performed. Conversion from column-integrated NH_3 to surface concentrations is omitted to minimize uncertainties linked to assumed vertical distributions, boundary layer dynamics, and gas–aerosol partitioning. To characterize IASI sensitivity, we use the random uncertainty associated with the retrieved NH_3 total column, as it provides a reliable proxy for the instrument's sensitivity [Clarisse et al., 2023].

Ground-based NH_3 measurements and IASI satellite observations are aggregated across multiple temporal (hourly to seasonal) and spatial scales (pixel level and circular averages with radii of 20–100 km, Figure 2). Two complementary approaches are implemented: (i) a pixel-based method using direct co-location of satellite and in situ observations, and (ii) a spatial averaging method where satellite data are averaged within circular areas of 20, 40, 60, and 100 km radius centered on monitoring sites. Relationships between surface concentrations and satellite-derived total columns are quantified using the Pearson correlation coefficient value, complemented by weighted linear regressions based on IASI random uncertainties to account for satellite sensitivity. The analysis is limited to IASI morning observations, corresponding to the period of maximum satellite sensitivity [Clarisse et al., 2023; Van Damme et al., 2018]. To ensure the robustness of the inter-comparisons between the IASI satellite and surface NH_3 datasets, the number of IASI contributing pixels and the related mean random uncertainty are taken into account. Seasonal analyses (winter: December-January-February, spring: March-April-May, summer: June-July-August, and autumn: September-October- November) are conducted separately to characterize seasonal variability in the relationship between surface NH_3 concentrations and satellite observations.

https://doi.org/10.5194/egusphere-2026-3909
Preprint. Discussion started: 24 July 2026

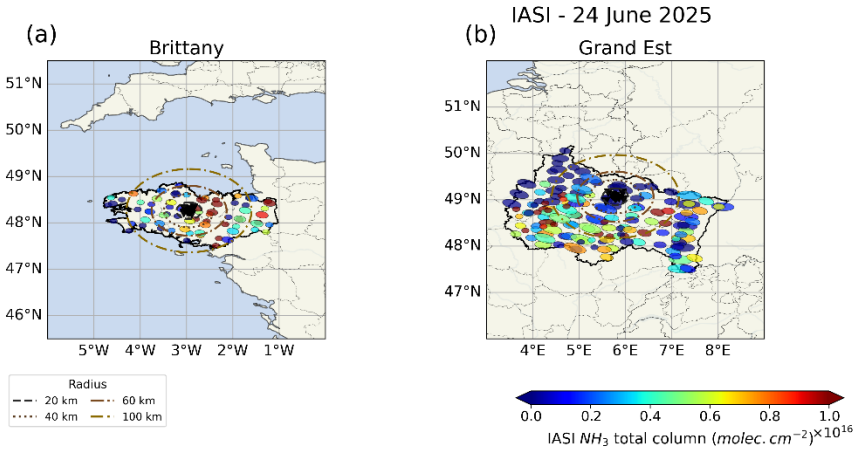

Figure 2: Example of maps of morning IASI pixels on 24 June 2025 for the 3 regions of interest. The locations of passive samplers and analyzers are indicated by black markers.

3 Results

3.1 Surface NH_3 concentration variabilities during the ROSAS campaign

Before addressing the comparisons of NH_3 concentrations derived by IASI and surface observations during the one-year ROSAS campaign (June 2024-June 2025), spatial variabilities of NH_3 concentrations are analyzed across the 3 regions according to their site influences (background, rural, cropland, livestock, and traffic, Figure 3).

On an annual basis, surface NH_3 concentrations are systematically higher at sites directly influenced by agricultural activities (livestock, fertilizer application, and rural environments) than at background sites. Agricultural sites typically exhibit mean concentrations exceeding ~3–10 $\mu g.m^{-3}$, whereas background sites generally remain below ~2 $\mu g.m^{-3}$. The traffic-influenced site in central Lyon (A-A-AURA and P-A-AURA) shows intermediate levels, with annual mean concentrations on the order of ~2–3 $\mu g.m^{-3}$.

A similar gradient is observed in spring, with background stations—particularly in the Auvergne–Rhône-Alpes region—recording concentrations below 2.5 µg.m-3, while agricultural sites frequently exceed 4 µg.m-3 during this period. This seasonal contrast reflects the intensification of agricultural practices in spring, notably fertilizer application and manure spreading.

In winter and autumn, NH_3 concentrations measured at the traffic-influenced site in central Lyon (A-A-AURA and P-A-AURA) are high and rank 6th to 8th among all sites, occasionally exceeding levels observed at some agricultural and rural locations. This suggests that road traffic may contribute to local NH_3 concentrations, although its role remains uncertain and is likely underestimated [Farren et al., 2020]. In summer, the traffic site ranks 5th, indicating relatively higher NH_3 concentrations compared to other locations. This increase may be partly associated with enhanced traffic activity, potentially linked to seasonal variations in vehicle flows along the nearby A7 highway during national summer holidays (within ~3 km

https://doi.org/10.5194/egusphere-2026-3909
Preprint. Discussion started: 24 July 2026

of the station, https://www.urbalyon.org/sites/default/storage_files/productions/publications/imports/2020-06/E-11383.pdf). However, the contribution of traffic relative to other sources cannot be clearly isolated based on the present analysis.

Overall, these results indicate that agricultural emissions dominate the variability of surface NH_3 concentrations across the three regions, with differences between site types reaching several $\mu g.m^{-3}$, especially during the spring peak.

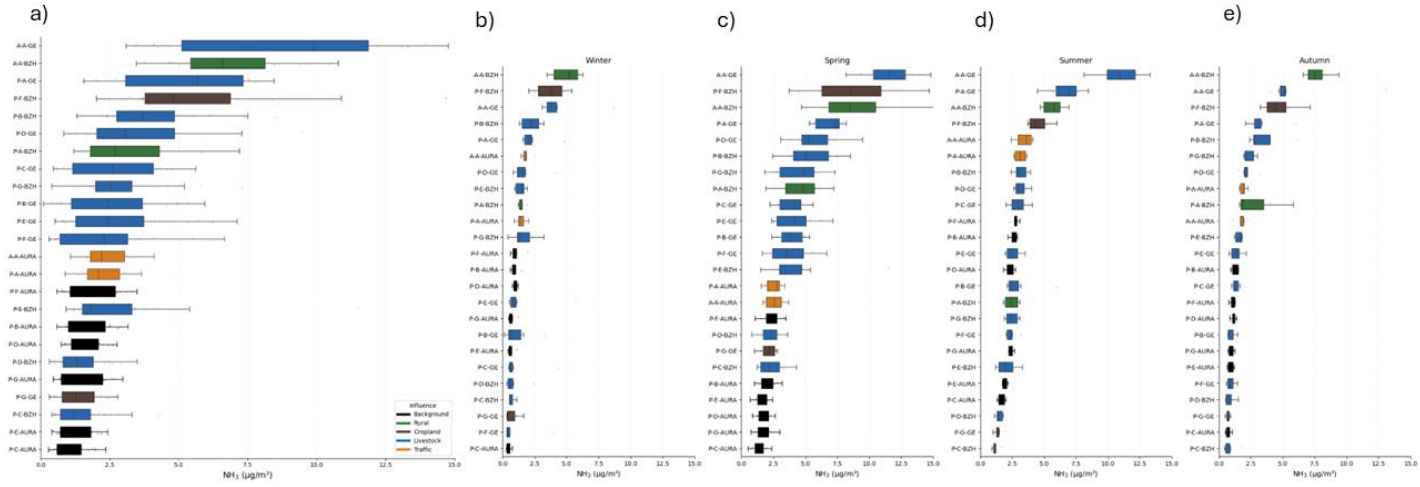

Figure 3: Statistic distribution of observed NH_3 surface concentrations averaged during the 1-year ROSAS field campaign between June 2024 and June 2025 (a), and for the different seasons: winter (b), spring (c), summer (d), and autumn (e). The different colors represent the a priori environmental incidence estimated per station.

3.2 Wind influence on surface NH_3 concentration variabilities

Having identified the influence of local sources on surface NH_3 concentrations, we further investigate the role of wind fields in driving NH_3 variability to better distinguish transported contributions from local emissions (Figure 4).

In Brittany, a consistent southwest–northeast gradient in surface NH_3 concentrations is observed across all seasons, aligned with prevailing wind directions. The magnitude of these spatial gradients ranges from 3 to 4 $\mu g.m^{-3}$ in winter, summer, and autumn, and reaches up to 7 $\mu g.m^{-3}$ in spring. The stronger spatial heterogeneity in spring suggests the influence of nearby local sources, particularly at site P-F-BZH, which records seasonal concentrations up to 8.9 $\mu g.m^{-3}$ in spring. According to the emission inventory, land use within a 1 km radius of the site is dominated by grasslands (~70%), including 39% permanent grasslands where fertilizer application is permitted year-round in France, together with corn cultivation, which requires substantial nitrogen fertilization during spring.

In the Grand Est region, the central site (A-A-GE and P-A-GE) consistently exhibits higher NH_3 concentrations across all seasons, indicating the presence of a local emission source. In contrast to Brittany, prevailing wind directions do not appear to strongly control spatial variability, as concentration gradients do not align with dominant wind patterns. In March, corresponding to fertilizer application periods, NH_3 concentrations approximately twice those observed in February across all sites, highlighting both regional and local influences of agricultural activities.

https://doi.org/10.5194/egusphere-2026-3909
Preprint. Discussion started: 24 July 2026

In Auvergne–Rhône-Alpes, spatial variability in NH_3 concentrations is limited (maximum differences <1.5 µg.m^{-3}) across all seasons, despite prevailing north–south wind patterns. These weak gradients suggest a dominant regional background influence. However, the central Lyon site (A-A-AURA and P-A-AURA) consistently records higher concentrations than surrounding sites, particularly in summer, indicating a likely contribution from road traffic emissions in this region, which is less influenced by agricultural activities.

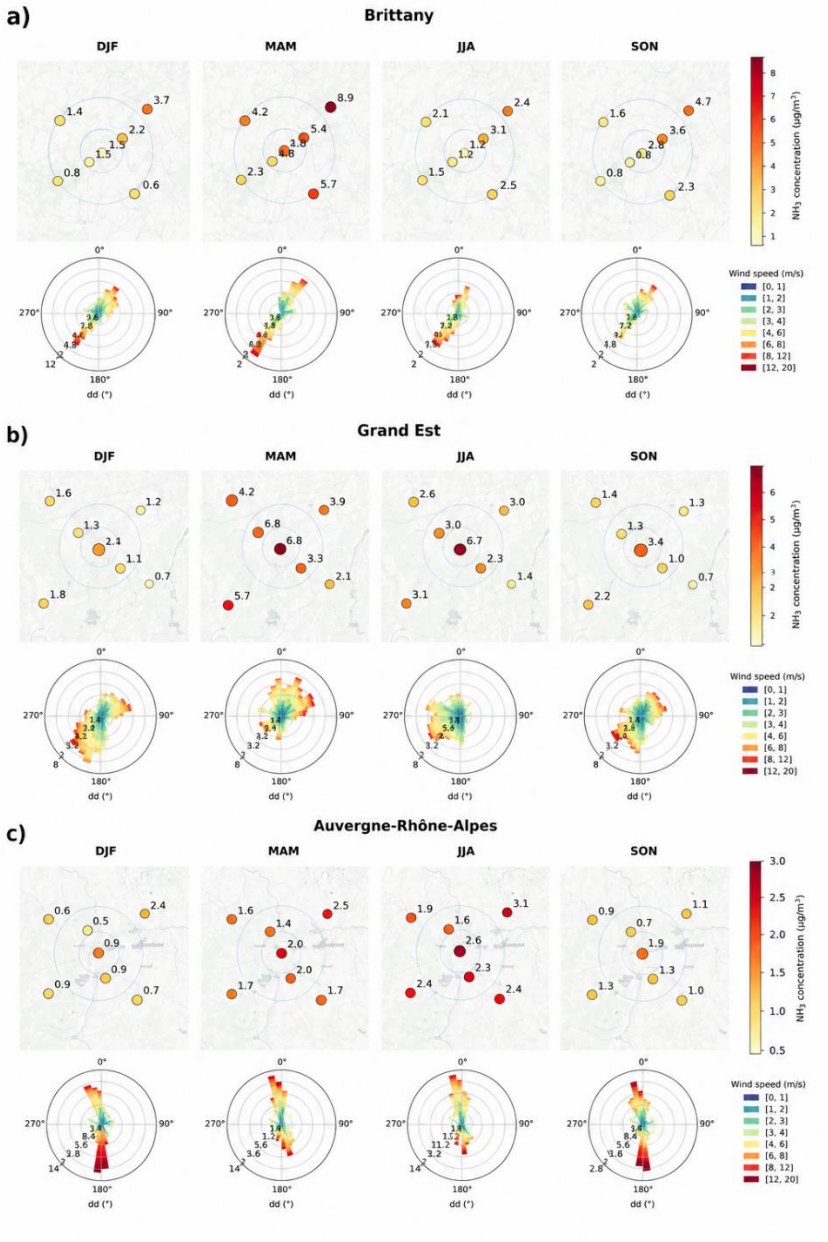

Figure 4: Seasonal average of NH_3 concentrations measured by passive samplers (upper panels) from June 2024 to June 2025, along with wind roses measured at the center of each region (lower panel) for Brittany (a), Grand Est (b), and Auvergne-Rhône-Alpes (c).

https://doi.org/10.5194/egusphere-2026-3909
Preprint. Discussion started: 24 July 2026

3.3 Representativeness of NH_3 surface measurements across each region

After analyzing the spatial variability of NH_3 with respect to emission source influences and regional wind patterns, we investigate the spatial representativeness of surface measurements within a 15 km radius for each region. As illustrated in Figure 5, clear differences in statistical distributions are observed across the three regions, reflecting contrasting regional emissions. Variability is expressed as the range (minimum-maximum) or interquartile range (Q1-Q3) of NH_3 concentrations measured within a 15km spatial extent across regions.

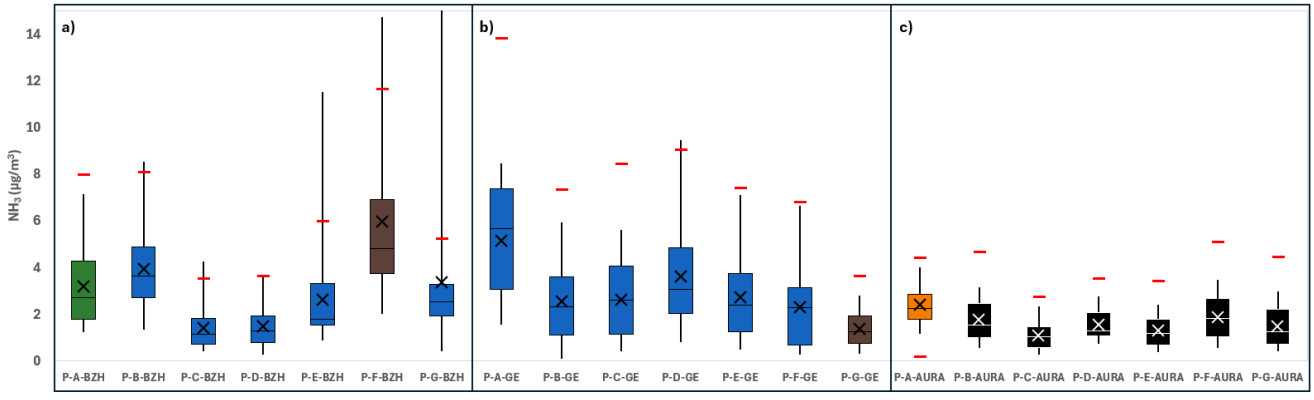

Figure 5: Box-plots of surface NH_3 concentrations measured during the ROSAS campaign in Brittany (a), Grand Est (b), and Auvergne-Rhône-Alpes (c) regions. The whiskers represent the minimum and maximum values, the box edges correspond to the first and third quartiles, the horizontal line within the box indicates the median, and the cross denotes the mean. Outlier thresholds (red lines) are defined according to the empirical rule of 1.5 × (Q3 − Q1) relative to the nearest quartile.

When averaged over a 15km radius, biweekly NH_3 concentrations measured by surface passive tubes averaged over the one-year period are 3.20 (1.43-5.98), 2.91 (1.38-5.16), and 1.65 (1.10-2.43) $\mu g.m^{-3}$ in Brittany, Grand Est, and AURA respectively. In Brittany, concentrations exhibit large variability, with wide interquartile ranges and frequent high maxima exceeding the outlier threshold. Sites C, D, and G show relatively compact distributions (Q3 − Q1 ~ 1.2 $\mu g.m^{-3}$), whereas sites A, B, and F are more variable (Q3 − Q1 > 2.1 $\mu g.m^{-3}$), with site E showing intermediate variability (~1.8 $\mu g.m^{-3}$). Elevated maxima are consistent with intensive agricultural practices (e.g., manure spreading), suggesting that extreme values reflect episodic emissions rather than statistical anomalies.

In the Grand Est region, variability remains substantial, but distributions are more constrained, with shorter whiskers and interquartile ranges around 2.5 $\mu g.m^{-3}$ (up to 4.3 $\mu g.m^{-3}$ at site A). Most sites (B–F) exhibit similar behavior, while sites A and G differ, the former showing high variability and the latter consistently low concentrations. The low values at site G are consistent with its local environmental characteristics.

In Auvergne–Rhône-Alpes, the urban site of Lyon displays limited variability (Q3 − Q1 < 1.6 $\mu g.m^{-3}$) and relatively low concentrations (maxima < 4 $\mu g.m^{-3}$), with no values exceeding the outlier threshold.

The observed differences between regions highlight the strong influence of local emission sources and land-use practices on NH_3 concentrations variability. Intensive livestock regions (e.g. Brittany) are characterized by high variability and elevated

https://doi.org/10.5194/egusphere-2026-3909
Preprint. Discussion started: 24 July 2026

maxima, whereas mixed or crop-dominated environments (e.g. Grand Est) show moderate variability with more constrained extrema. Urban areas (e.g. AURA) exhibit low variability and low concentrations, reflecting more diffuse emission sources.

3.4 Characterization of IASI NH_3 observations over the 3 regions

To assess the representativeness of surface NH_3 measurements in support of IASI satellite observations, IASI dataset is first characterized over the three study regions for the 2018–2025 period and for the ROSAS campaign period (S2). The objective is to evaluate whether NH_3 concentrations, retrieval random uncertainties, and pixel sampling during the campaign are representative of longer-term regional conditions.

IASI NH_3 column distributions are broadly consistent across regions with comparable values ranging from 2.10^{16} to 3.10^{16} molec.cm^{-2} (Figure S2a), although Brittany exhibits greater dispersion, with a median of approximately 7.10^{15} molec.cm^{-2} during the ROSAS field campaign. The Grand Est region shows intermediate variability (centered around a median of ~6.10^{15} molec.cm^{-2}), while Auvergne–Rhône-Alpes displays a more constrained distribution centered around a lower median (~5.10^{15} molec.cm^{-2}). These differences likely reflect contrasts in NH_3 emission sources, particularly stronger agricultural activity in Brittany, as well as meteorological conditions and the spatial structure of emissions. Random uncertainties associated with IASI NH_3 observations (Figure S2b) indicates comparable levels across regions, with slightly lower uncertainties in Auvergne–Rhône-Alpes. Number of available pixels per day (Figure S2c) varies significantly between regions, with Grand Est and Auvergne–Rhône-Alpes generally showing higher pixel counts than Brittany. This difference can be attributed to variations in regional extent and satellite observation conditions, which affect pixel availability. Comparison between the campaign period and the longer-term record indicates similar distributions, suggesting that the campaign observations are representative of multi-year variability.

During the ROSAS campaign, the monthly mean NH_3 columns measured by IASI showed a marked seasonal cycle across the three regions (Figure 6), with elevated values in spring (March–April) and summer and lows in cold months (minimum in November–January) consistent with agricultural emission patterns. In Brittany, the columns ranged from 1.44×10^{15} mol. cm^{-2} in February 2025 to 1.26×10^{16} mol. cm^{-2} in April 2025. In the Grand Est region, they reached a maximum of 1.18×10^{16} mol. cm^{-2} in March 2025, compared to a minimum of 1.11×10^{14} mol. cm^{-2} in December 2024. In the Auvergne-Rhône-Alpes region, the values ranged from 9.27×10^{14} to 1.04×10^{16} mol. cm^{-2}, with a maximum in June 2025. Surface NH_3 concentrations measured by analyzers show generally similar temporal variations, with values ranging from 2.63 to 7.65 µg.m^{-3} in Brittany and from 1.42 to 3.95 µg.m^{-3} in Auvergne-Rhône-Alpes. The number of IASI pixels also varies by region, averaging 675 pixels per month in Brittany, compared to 1576 in Grand Est and 1891 in Auvergne-Rhône-Alpes, reflecting in particular Brittany's smaller surface area.

Despite regional differences and variations in satellite coverage, both IASI and surface datasets exhibit similar seasonal cycles. This overall consistency is further examined through the analysis of their spatiotemporal correlations.

https://doi.org/10.5194/egusphere-2026-3909
Preprint. Discussion started: 24 July 2026

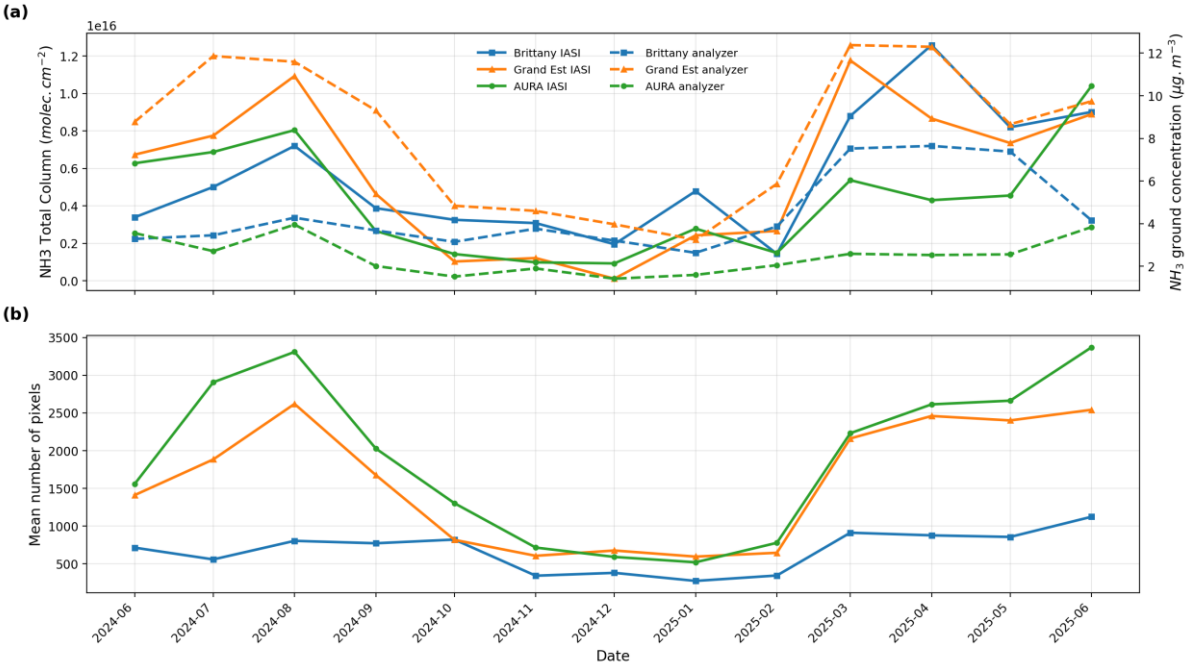

Figure 6: Temporal evolution of monthly mean NH_3 total columns from IASI across the three regions (solid lines, blue for Brittany, orange for Grand Est, and green for Auvergne-Rhône-Alpes) and monthly mean surface NH_3 concentrations measured by analyzers during the campaign (dashed lines) (a), along with the monthly total number of IASI pixels (b).

3.5 Assessment of the agreement between IASI and ground-based NH_3 measurements

The analysis of agreement and discrepancies between satellite and surface NH_3 measurements helps assess the importance of combining both approaches for NH_3 monitoring. When strong correlations are observed, satellite measurements are likely to be considered representative of surface conditions, while ground-based observations contribute to their validation. Conversely, weak correlations indicate that surface measurements capture local variability and conditions that are not resolved by satellite observations. In such cases, in situ data provide complementary information at finer spatial scales.

In the context of this study, which compares surface-based measurements — both passive (biweekly integrated) and active (hourly) — with IASI total columns, correlation coefficients of 0.7 or above are considered indicative of satisfactory agreement (based on the literature, see Introduction Section). It is essential to ensure that the IASI satellite sensitivity (including random uncertainties) and data availability are sufficient to support meaningful comparisons. Temporal aggregation is subject to a data completeness criterion requiring at least 25% of expected observations (i.e., ≤75% missing data). Aggregations are performed at hourly, daily, weekly, monthly, seasonal, and biweekly scales. All correlations are shown in space–time diagrams; however, numerical annotations are restricted to robust results with statistical significance ($p \leq 0.05$).

https://doi.org/10.5194/egusphere-2026-3909
Preprint. Discussion started: 24 July 2026

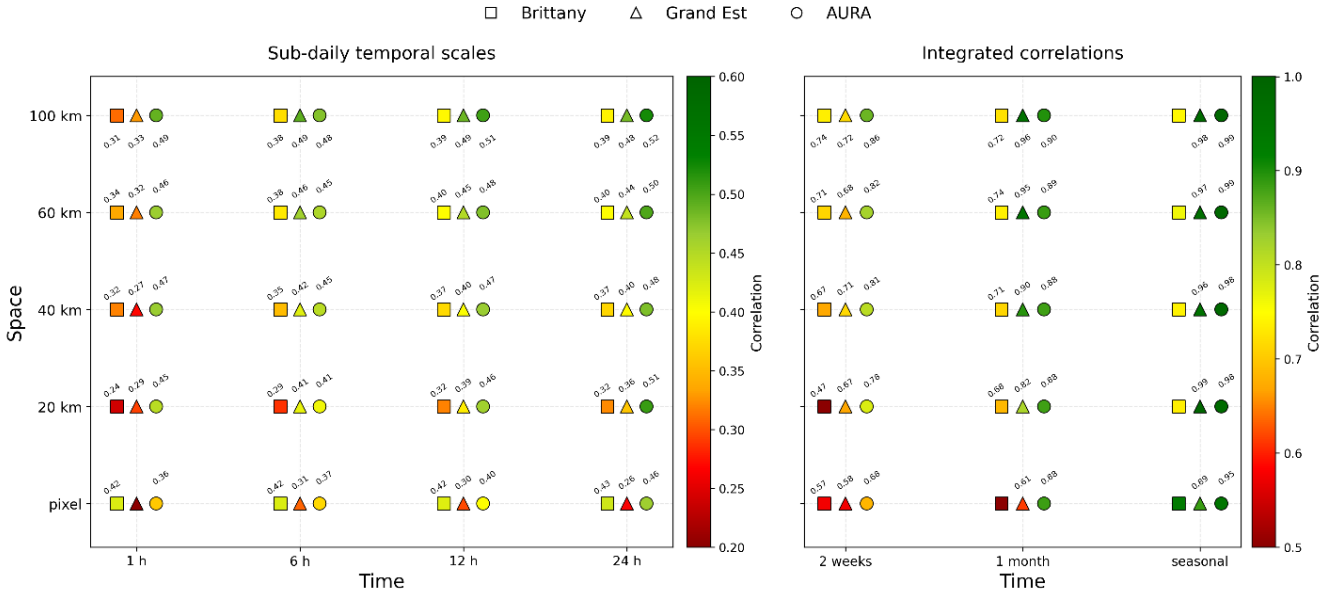

Figure 7: Space–time diagrams of color-coded Pearson correlation coefficient between IASI and surface NH_3 observations for Brittany (square), Grand Est (triangle), and Auvergne-Rhône-Alpes (circle) during the ROSAS campaign for sub-daily scales (hourly, 6 hours, 12 hours, and 24 hours, left panel) and for integrated measurements (2 weeks, 1 month, and seasonal, right panel). All correlations are displayed, but only those that are statistically significant (p-value < 0.05) are annotated.

As shown in Figure 7, NH_3 surface concentrations and IASI total columns show weak to moderate agreement across sub-daily temporal scales (1h, 6h, 12h, daily), with Pearson correlation coefficients (R) ranging from 0.24 to 0.52 (Figure 7). Agreement generally improves when integrating over more than 2 weeks (2 weeks, monthly, seasonally), with Pearson R ranging from 0.47 to 0.99. Part of this improvement can be attributed to the smaller number of paired observations included in the comparisons. Indeed, hourly to daily analyses are based on approximately 200–300 surface observations, whereas bi-weekly, monthly, and seasonal comparisons rely on only 29, 13, and 5 observations, respectively.

The number of IASI pixels numbers used in the comparisons increases by a factor of ~200 between 20 km and 100 km, resulting in improved agreement due to reduced retrieval uncertainties from spatial averaging. For example, at a biweekly timescale, 29 ground-based observations are available in Brittany and the Pearson correlation coefficient increases from R = 0.47 (290 pixels, 20 km) to 0.67 (1271 pixels, 40 km). Across spatial scales from 20 to 100 km, correlation coefficients increase from 0.47 to 0.74 (+0.27) in Brittany, from 0.67 to 0.72 (+0.05) in Grand Est, and from 0.78 to 0.86 (+0.08) in Auvergne–Rhône-Alpes. Notably, in Brittany, correlations values improve by +0.20 when increasing the number of pixels from 290 (20 km) to 1271 (40 km) whereas only minor improvements are observed in Grand Est (+0.04) and Auvergne–Rhône-Alpes (+0.03). This enhancement in Brittany primarily reflects noise reduction due to increased IASI pixel sampling. These results suggest that increasing the number of satellite pixels included in the comparison reduces noise in IASI measurements and

https://doi.org/10.5194/egusphere-2026-3909
Preprint. Discussion started: 24 July 2026

improves agreement with surface observations. This also highlights the importance of including a sufficient number of pixels to reduce noise in IASI observations and to ensure that agreement metrics are based on comparable sample sizes.

The analysis of temporal scales at which the best agreement is found between IASI and surface NH_3 concentrations could provide insight into atmospheric NH_3 processes. In Brittany, for a comparable number of pixels at 20 km (~ 350), the highest correlation (R = 0.32) is obtained when surface observations are averaged over 12–24 h around the satellite overpass. In the Grand Est region, at a 20 km scale and for a similar number of pixels (~ 442), the best agreement (R = 0.41) is achieved using 6 h averages of surface observations, indicating a potential influence of short-term variability in local emissions. In Auvergne–Rhône-Alpes, at 20 km (~ 452 pixels), the highest correlation (R = 0.51) is obtained using daily averages, suggesting weaker temporal variability of local sources in this region. Overall, the highest correlations are obtained using daily averages of surface observations in Auvergne–Rhône-Alpes, 12–24 h averages in Brittany, and 6 h averages in Grand Est, suggesting weaker temporal variability of local sources in Auvergne–Rhône-Alpes, moderate NH_3 variability in Brittany, and stronger variability in Grand Est.

We further examine the representativeness of surface measurements with regards to satellite observations. For this, we first assess agreement, quantified by Pearson correlation coefficients, between IASI observations with NH_3 concentrations derived from the analyzer (centered in each region), the passive tubes, and the average of all surface measurements (e.g. ground average) computed over a 2-week period (Supplement information S3). Results show that over Brittany, Pearson coefficient correlations between IASI and surface measurements increase by +0.10 at all scales (from 20 to 100 km) when comparing with the analyzer compared to temporal integrated ground measurements (passive tube and ground average). In contrast, NH_3 concentrations derived from the analyzer show poorer agreement with IASI compared to temporally integrated measurements (passive tubes and ground average) over Auvergne-Rhône-Alpes. For Grand Est, agreement is very similar when using the ground mean of surface measurements, the passive tubes and the analyzer.

We also analyzed which passive sampling sites show the strongest agreement with IASI across regions, using a temporal window of 2 weeks and a spatial criterion of 20km (Table S4). In Brittany, correlations between IASI and the different surface sites show large variability across sites (R = 0.32–0.66), with the highest agreement observed at sites P-B-BZH and P-F-BZH, characterized by low to intermediate NH_3 concentrations. This suggests that, in heterogeneous and high-emission regions, such as Brittany, sites with intermediate concentrations are more representative of satellite observations. In the Grand Est region, variability across sites is more limited (R = 0.59–0.80), with several sites (P-F-GE, P-C-GE, and P-G-GE) showing strong agreement with IASI ($R \geq 0.7$). In Auvergne–Rhône-Alpes, correlations are uniformly high (R = 0.79–0.86), with the strongest agreement observed at the central Lyon site.

We now examine the agreement between ground-based and satellite NH_3 measurements per season (Figure 8). In winter, agreement between surface NH_3 concentrations and IASI columns is generally weaker, with almost no significant values (p-

https://doi.org/10.5194/egusphere-2026-3909
Preprint. Discussion started: 24 July 2026

values are > 0.05) across all regions, with the highest correlations observed in the Grand Est region. This likely reflects both low NH_3 concentrations (<5 µg.m^{-3}; Figure 2) and increased noise in IASI retrievals, partly due to reduced thermal contrast. In spring, good correlations (R ~0.5) are observed in Grand Est and Auvergne–Rhône-Alpes when IASI observations are averaged within a 40 km radius. When the spatial window is reduced to 20 km, a good agreement is maintained at hourly resolution, suggesting the influence of intermittent agricultural activities (e.g., fertilizer application). Overall, in all regions during spring, agreement with IASI improves as the spatiotemporal averaging scales increase, suggesting a stronger influence of regionally transported NH_3. In autumn, moderate agreement (0.41-0.49) is found in Auvergne–Rhône-Alpes across all temporal scales when considering spatial windows of 40 km and larger. In summer, strong agreement is observed in Brittany across all spatial and temporal scales, including at the nearest IASI pixel when using 12 or 24 h averages. Elevated NH_3 concentrations measured by both IASI and surface analyzers likely contribute to these high correlations. In Grand Est, correlations are moderate overall but consistently improve when the temporal averaging window is reduced to 6 h. In Auvergne–Rhône-Alpes, the best agreement is obtained at larger spatiotemporal scales (100 km, daily).

Figure 8: Space–time diagrams of color-coded Pearson correlation coefficient between IASI and surface NH_3 observations for Brittany (square), Grand Est (triangle), and Auvergne-Rhône-Alpes (circle) during the ROSAS campaign for sub-daily scales (hourly, 6 hours, 12 hours, and 24 hours, left panel), break by season during the ROSAS campaign. All correlations are displayed, but only those significant (p-value < 0.05) ones are annotated.

https://doi.org/10.5194/egusphere-2026-3909
Preprint. Discussion started: 24 July 2026

4 Conclusions

This study investigates the complementarity between IASI satellite observations and ground-based NH_3 measurements across major French agricultural regions to determine the spatiotemporal scales at which satellite observations reliably capture surface NH_3 variability. By analyzing the representativeness and correlation of both datasets, this study aims to improve the integration of satellite and in situ observations for ammonia air quality monitoring and emission mitigation strategies.

For one year (June 2024 to June 2025), a total of 24 surface NH_3 measurement sites were deployed across the three highest-emitting regions of France (Brittany, Grand Est, and Auvergne-Rhône-Alpes), with sites in each region distributed within a 15-km spatial extent in the frame of the ROSAS campaign. Information on local emission sources was used to classify the dominant influence at each site. On an annual basis, NH_3 concentrations at agricultural sites are higher and more variable than at background sites, while traffic-influenced sites exhibit intermediate levels.

Surface NH_3 concentrations exhibit region-specific spatial patterns, with strong wind-aligned gradients and local sources influence in Brittany (particularly in spring), uniformed enhancements linked to agricultural activities in Grand Est, and relatively homogeneous regional background levels in Auvergne–Rhône-Alpes, except for elevated concentrations at the urban Lyon site likely influenced by traffic emissions.

IASI-derived NH_3 total columns exhibit similar distributions across regions, with greater variability in Brittany associated with agricultural emissions, while uncertainties remain comparable and slightly lower in Auvergne–Rhône-Alpes. The number of available pixels varies by region, but overall, satellite observations capture interannual variability well, providing a robust basis for comparisons between surface measurements and satellite data.

Satellite-derived monthly NH_3 columns exhibit a pronounced seasonal cycle, with maxima in spring and summer consistent with agricultural emission periods, and minima during winter. Surface analyzer measurements show similar temporal variations, and despite regional differences and variations in satellite coverage, both datasets display an overall temporal consistency prior to the analysis of their spatiotemporal correlations.

IASI and surface NH_3 observations agreements have been assessed across various spatiotemporal scales to infer the importance of combining both approaches for NH_3 monitoring.

IASI NH_3 columns and surface analyzer concentrations show strong correlations at monthly and seasonal scales; however, this largely reflects the limited number of data points (13 months and 5 seasons). Robust agreement ($R \geq 0.7$), ensuring sufficient numbers of points in the comparison, is also achieved at a biweekly scale when averaging all IASI pixels within a 20-40 km radius around the station, indicating that IASI could effectively support NH_3 surface monitoring at ~20-40 km spatial resolution on a two-week timescale.

Relationships between IASI columns and surface analyzer measurements are generally weak to moderate at daily and sub-daily timescales. This may indicate that IASI, with a fixed overpass time around 09:30, has limited capability to capture intra- to inter-day variability in surface NH_3, potentially due to reduced sensitivity near the surface compared with in situ measurements.

https://doi.org/10.5194/egusphere-2026-3909
Preprint. Discussion started: 24 July 2026

However, the temporal averaging window yielding the highest correlations provides insight into regional NH_3 variability: in Grand Est, optimal agreement is obtained using 6 h averages around the satellite overpass, suggesting rapid and pronounced temporal variability, whereas in Auvergne–Rhône-Alpes and Brittany, better agreement is achieved with 12 h to daily averaging, indicating more stable or slower temporal variations in NH_3 concentrations.

Careful site selection is essential, taking into account local emission sources and wind patterns. In heterogeneous, high-emission regions (e.g., Brittany), surface measurements should include both sites representative of average NH_3 concentrations, which are better correlated with satellite observations, and sites located near point sources to capture additional local variability. In particular, ground-based instrumentation is required to characterize localized or highly variable sources that are not adequately captured by satellites, such as road traffic or point emissions.

These results suggest that satellite observations are well suited for long-term monitoring of NH_3, including bi-weekly, seasonal, and trend analyses, provided they are supported by targeted ground-based measurements (e.g., passive samplers) for validation. However, investigating fine-scale processes at spatial (<40 km) and temporal (<daily) scales, surface measurements remain essential to complement satellite data.

The upcoming geostationary InfraRed Sounder (IRS) mission (launched in summer 2025) is expected to significantly enhance spatial and temporal resolution compared to IASI (from ~12 km to a few kilometers, e.g., ~ 4 × 7 km over Brittany, with a revisit time of ~ 30 min). This enhanced capability complements dense surface measurement networks, which remain essential for accurate air quality monitoring.

https://doi.org/10.5194/egusphere-2026-3909
Preprint. Discussion started: 24 July 2026

Data availability

- Reanalyzed Metop-A: https://www.aeris-data.fr/en/landing-page/?uuid=871d9366-22d7-4d8d-997e-02e7721f7e94

Clarisse, L. & Coheur, P.-F. (2018). Reanalyzed daily IASI/Metop-A ULB-LATMOS ammonia (NH3) L2 product (total column). [dataset]. Aeris. https://doi.org/10.25326/12

- Reanalyzed Metop-B: https://www.aeris-data.fr/en/landing-page/?uuid=44a739bf-8b68-4b64-b594-d7bb3fbe40bf

Clarisse, L. & Coheur, P.-F. (2018). Reanalyzed daily IASI/Metop-B ULB-LATMOS ammonia (NH3) L2 product (total column). [dataset]. Aeris. https://doi.org/10.25326/13

- Reanalyzed Metop-C: https://www.aeris-data.fr/en/landing-page/?uuid=fa819000-2a14-4059-9cb7-963d36e98c3c

Clarisse, L. & Coheur, P.-F. (2020). Reanalyzed daily IASI/Metop-C ULB-LATMOS ammonia (NH3) L2 product (total column). [dataset]. Aeris. https://doi.org/10.25326/500

Author contributions

CV, VL, AC, MD, MC, MB, J L-P, JC, and G S-G designed the experiments. CV, VL, AC, MD, MC, MB, A L-L, and G S-M analysed the dataset. CV prepared the manuscript with contributions from all co-authors. A L-L reviewed the manuscript.

Competing interests

The contact author has declared that none of the authors has any competing interests.

Acknowledgements

The completion of this study was made possible through the combined support of several infrastructures and collaborations. IASI observations were accessed via the AERIS data infrastructure (https://www.aeris-data.fr/), NH_3 retrievals were developed by the ULB–LATMOS collaboration, and the NH_3 products were provided through the EUMETSAT Atmospheric Composition Satellite Application Facility (AC SAF; http://acsaf.org). IASI is a joint mission of EUMETSAT and the Centre National d'Etudes Spatiales (CNES; France). The IASI Level 1C data are distributed in near-real time by EUMETSAT through the EUMETCast system distribution. The authors would like to thank Anne Boynard and Nadir Guendouz from LATMOS for their careful reviews of the manuscript and for their valuable suggestions, which greatly improved the quality of the writing.

https://doi.org/10.5194/egusphere-2026-3909
Preprint. Discussion started: 24 July 2026

Financial support

This work has been funded by the french Agence de l'Environnement et de la Maîtrise de l'Energie (ADEME) in the frame of the Amélioration de la Qualité de l'Air : Comprendre, Innover, Agir (AQACIA) program, grant number 2262D0091.

References

Aneja, V. P., Schlesinger, W. H., Li, Q., Nahas, A. and Battye, W. H.: Characterization of the Global Sources of Atmospheric Ammonia from Agricultural Soils, J. Geophys. Res. Atmos., 125(3), e2019JD031684, doi:https://doi.org/10.1029/2019JD031684, 2020.

Azim, R. M. and Torii, S.: Exploring the potential of ammonia and hydrogen as alternative fuels for transportation, 14(1), doi:doi:10.1515/eng-2024-0024, 2024.

Beaudor, M., Hauglustaine, D., Lathière, J., Van Damme, M., Clarisse, L. and Vuichard, N.: Evaluating present-day and future impacts of agricultural ammonia emissions on atmospheric chemistry and climate, Atmos. Chem. Phys., 25(4), 2017–2046, doi:10.5194/acp-25-2017-2025, 2025.

Berkhout, A. J. C., Swart, D. P. J., Volten, H., Gast, L. F. L., Haaima, M., Verboom, H., Stefess, G., Hafkenscheid, T. and Hoogerbrugge, R.: Replacing the AMOR with the miniDOAS in the ammonia monitoring network in the Netherlands, Atmos. Meas. Tech., 10(11), 4099–4120, doi:10.5194/amt-10-4099-2017, 2017.

Bleeker, A., Sutton, M. A., Acherman, B., Alebic-Juretic, A., Aneja, V. P., Ellermann, T., Erisman, J. W., Fowler, D., Fagerli, H., Gauger, T., Harlen, K. S., Hole, L. R., Horvath, L., Mitosinkova, M., Smith, R. I., Tang, Y. S. and van Pul, A.: Linking Ammonia Emission Trends to Measured Concentrations and Deposition of Reduced Nitrogen at Different Scales BT - Atmospheric Ammonia: Detecting emission changes and environmental impacts, edited by M. A. Sutton, S. Reis, and S. M. H. Baker, pp. 123–180, Springer Netherlands, Dordrecht., 2009.

Buijsman, E., Aben, J. M. M., Van Elzakker, B. G. and Mennen, M. G.: An automatic atmospheric ammonia network in the Netherlands set-up and results, Atmos. Environ., 32(3), 317–324, doi:https://doi.org/10.1016/S1352-2310(97)00233-1, 1998.

Cao, H., Henze, D. K., Shephard, M. W., Dammers, E., Cady-Pereira, K., Alvarado, M., Lonsdale, C., Luo, G., Yu, F., Zhu, L., Danielson, C. G. and Edgerton, E. S.: Inverse modeling of NH_3 sources using CrIS remote sensing measurements, Environ. Res. Lett., 15(10), 104082, doi:10.1088/1748-9326/abb5cc, 2020.

Clarisse, L., Franco, B., Van Damme, M., Di Gioacchino, T., Hadji-Lazaro, J., Whitburn, S., Noppen, L., Hurtmans, D., Clerbaux, C. and Coheur, P.: The IASI NH_3 version 4 product: averaging kernels and improved consistency, Atmos. Meas. Tech., 16(21), 5009–5028, doi:10.5194/amt-16-5009-2023, 2023.

Clerbaux, C., Boynard, A., Clarisse, L., George, M., Hadji-Lazaro, J., Herbin, H., Hurtmans, D., Pommier, M., Razavi, A., Turquety, S., Wespes, C. and Coheur, P.-F.: Monitoring of atmospheric composition using the thermal infrared IASI/MetOp sounder, Atmos. Chem. Phys., 9(16), 6041–6054, doi:10.5194/acp-9-6041-2009, 2009.

https://doi.org/10.5194/egusphere-2026-3909
Preprint. Discussion started: 24 July 2026

Cheng, B., Wang-Li, L., Meskhidze, N., Classen, J. and Bloomfield, P.: Partitioning of NH_3-NH4+ in the Southeastern U.S., Atmosphere (Basel)., 12(12), doi:10.3390/atmos12121681, 2021.

Dammers, E., McLinden, C. A., Griffin, D., Shephard, M. W., Van Der Graaf, S., Lutsch, E., Schaap, M., Gainairu-Matz, Y., Fioletov, V., Van Damme, M., Whitburn, S., Clarisse, L., Cady-Pereira, K., Clerbaux, C., Coheur, P. F. and Erisman, J. W.: NH_3 emissions from large point sources derived from CrIS and IASI satellite observations, Atmos. Chem. Phys., 19(19), 12261–12293, doi:10.5194/acp-19-12261-2019, 2019.

Dammers, E., Shephard, M. W., Palm, M., Cady-Pereira, K., Capps, S., Lutsch, E., Strong, K., Hannigan, J. W., Ortega, I., Toon, G. C., Stremme, W., Grutter, M., Jones, N., Smale, D., Siemons, J., Hrpcek, K., Tremblay, D., Schaap, M., Notholt, J. and Erisman, J. W.: Validation of the CrIS fast physical NH_3 retrieval with ground-based FTIR, Atmos. Meas. Tech., 10(7), 2645–2667, doi:10.5194/amt-10-2645-2017, 2017.

Dammers, E., Palm, M., Van Damme, M., Vigouroux, C., Smale, D., Conway, S., Toon, G. C., Jones, N., Nussbaumer, E., Warneke, T., Petri, C., Clarisse, L., Clerbaux, C., Hermans, C., Lutsch, E., Strong, K., Hannigan, J. W., Nakajima, H., Morino, I., Herrera, B., Stremme, W., Grutter, M., Schaap, M., Wichink Kruit, R. J., Notholt, J., Coheur, P.-F. and Erisman, J. W.: An evaluation of IASI-NH_3 with ground-based Fourier transform infrared spectroscopy measurements, Atmos. Chem. Phys., 16(16), 10351–10368, doi:10.5194/acp-16-10351-2016, 2016.

da Silva, E. A., Samuel, C., Furini, L. N., Constantino, C. J. L., Redon, N. and Duc, C.: Poly(aniline)-based ammonia sensors: Understanding the role of polyurethane on structural/morphological properties and sensing performances, Sensors Actuators B Chem., 397, 134664, doi:https://doi.org/10.1016/j.snb.2023.134664, 2023.

Ding, J., van der A, R., Eskes, H., Dammers, E., Shephard, M., Wichink Kruit, R., Guevara, M. and Tarrason, L.: Ammonia emission estimates using CrIS satellite observations over Europe, Atmos. Chem. Phys., 24(18), 10583–10599, doi:10.5194/acp-24-10583-2024, 2024.

Ellis, R. A., Murphy, J. G., Pattey, E., van Haarlem, R., O'Brien, J. M. and Herndon, S. C.: Characterizing a Quantum Cascade Tunable Infrared Laser Differential Absorption Spectrometer (QC-TILDAS) for measurements of atmospheric ammonia, Atmos. Meas. Tech., 3(2), 397–406, doi:10.5194/amt-3-397-2010, 2010.

European Environment Agency (2024). DIRECTIVE (EU) 2024/2881 OF THE EUROPEAN PARLIAMENT AND OF THE COUNCIL. Retrieved from https://eur-lex.europa.eu/legal-content/EN/TXT/HTML/?uri=OJ:L_202402881)

European Environment Agency (2020). European Union emission inventory report 1990-2018 under the UNECE Convention on long-range Transboundary Air Pollution (LRTAP). LU Publications Office. Retrieved from https://data.europa.eu/doi/10.2800/233574

Evangeliou, N., Balkanski, Y., Eckhardt, S., Cozic, A., Van Damme, M., Coheur, P.-F., Clarisse, L., Shephard, M. W., Cady-Pereira, K. E. and Hauglustaine, D.: 10-year satellite-constrained fluxes of ammonia improve performance of chemistry transport models, Atmos. Chem. Phys., 21(6), 4431–4451, doi:10.5194/acp-21-4431-2021, 2021.

Farren, N. J., Davison, J., Rose, R. A., Wagner, R. L. and Carslaw, D. C.: Underestimated Ammonia Emissions from Road Vehicles, Environ. Sci. Technol., 54(24), 15689–15697, doi:10.1021/acs.est.0c05839, 2020.

https://doi.org/10.5194/egusphere-2026-3909
Preprint. Discussion started: 24 July 2026

Guo, X., Wang, R., Pan, D., Zondlo, M. A., Clarisse, L., Van Damme, M., Whitburn, S., Coheur, P.-F., Clerbaux, C., Franco, B., Golston, L. M., Wendt, L., Sun, K., Tao, L., Miller, D., Mikoviny, T., Müller, M., Wisthaler, A., Tevlin, A. G., Murphy, J. G., Nowak, J. B., Roscioli, J. R., Volkamer, R., Kille, N., Neuman, J. A., Eilerman, S. J., Crawford, J. H., Yacovitch, T. I., Barrick, J. D. and Scarino, A. J.: Validation of IASI Satellite Ammonia Observations at the Pixel Scale Using In Situ Vertical Profiles, J. Geophys. Res. Atmos., 126(9), e2020JD033475, doi:https://doi.org/10.1029/2020JD033475, 2021.

Kim, K., Park, G., Kang, S., Singh, R., Song, J., Choi, S., Park, I., Yu, D.-G., Kim, M.-B., Bae, M.-S., Jung, S., Chang, Y., Park, J., Jung, H.-J., Lim, Y. and Lee, T.: The Comparisons of Real-time Ammonia Adsorption Measurement in Varying Inlet Tubes and the Different Ammonia Measurement Methods in the Atmosphere, Asian J. Atmos. Environ., 15(4), 2021139, doi:10.5572/ajae.2021.139, 2021.

Liu, X., Lara, R., Dufresne, M., Wu, L., Zhang, X., Wang, T., Monge, M., Reche, C., Di Leo, A., Lanzani, G., Colombi, C., Font, A., Sheehan, A., Green, D. C., Makkonen, U., Sauvage, S., Salameh, T., Petit, J.-E., Chatain, M., Coe, H., Hou, S., Harrison, R., Hopke, P. K., Petäjä, T., Alastuey, A. and Querol, X.: Variability of ambient air ammonia in urban Europe (Finland, France, Italy, Spain, and the UK), Environ. Int., 185, 108519, doi:https://doi.org/10.1016/j.envint.2024.108519, 2024.

Liu, S., Xu, H., Wang, J., Ding, J., Liu, P., Yang, Y. and Liu, L.: Evidence for global increases in urban ammonia pollution and their drivers, Sci. Total Environ., 955, 176846, doi:https://doi.org/10.1016/j.scitotenv.2024.176846, 2024.

Lolkema, D. E., Noordijk, H., Stolk, A. P., Hoogerbrugge, R., van Zanten, M. C. and van Pul, W. A. J.: The Measuring Ammonia in Nature (MAN) network in the Netherlands, Biogeosciences, 12(16), 5133–5142, doi:10.5194/bg-12-5133-2015, 2015.

Luo, Z., Zhang, Y., Chen, W., Van Damme, M., Coheur, P.-F. and Clarisse, L.: Estimating global ammonia (NH$_{3}$) emissions based on IASI observations from 2008 to 2018, Atmos. Chem. Phys., 22(15), 10375–10388, doi:10.5194/acp-22-10375-2022, 2022.

Ma, J., Shi, H., Zhu, Y., Li, R., Wang, S., Lu, N., Yao, Y., Bian, Z. and Huang, K.: The Evolution of Global Surface Ammonia Concentrations during 2001–2019: Magnitudes, Patterns, and Drivers, Environ. Sci. Technol., 59(10), 5066–5079, doi:10.1021/acs.est.4c14020, 2025.

Marais, E. A., Pandey, A. K., Van Damme, M., Clarisse, L., Coheur, P.-F., Shephard, M. W., Cady-Pereira, K. E., Misselbrook, T., Zhu, L., Luo, G. and Yu, F.: UK Ammonia Emissions Estimated With Satellite Observations and GEOS-Chem, J. Geophys. Res. Atmos., 126(18), e2021JD035237, doi:https://doi.org/10.1029/2021JD035237, 2021.

McDuffie, E. E., Smith, S. J., O'Rourke, P., Tibrewal, K., Venkataraman, C., Marais, E. A., Zheng, B., Crippa, M., Brauer, M. and Martin, R. V: A global anthropogenic emission inventory of atmospheric pollutants from sector- and fuel-specific sources (1970--2017): an application of the Community Emissions Data System (CEDS), Earth Syst. Sci. Data, 12(4), 3413–3442, doi:10.5194/essd-12-3413-2020, 2020.

Nair, A. A. and Yu, F.: Quantification of Atmospheric Ammonia Concentrations: A Review of Its Measurement and Modeling, Atmosphere (Basel)., 11(10), doi:10.3390/atmos11101092, 2020.

https://doi.org/10.5194/egusphere-2026-3909
Preprint. Discussion started: 24 July 2026

Shephard, M. W. and Cady-Pereira, K. E.: Cross-track Infrared Sounder (CrIS) satellite observations of tropospheric ammonia, Atmos. Meas. Tech., 8(3), 1323–1336, doi:10.5194/amt-8-1323-2015, 2015.

Shephard, M. W., Cady-Pereira, K. E., Luo, M., Henze, D. K., Pinder, R. W., Walker, J. T., Rinsland, C. P., Bash, J. O., Zhu, L., Payne, V. H. and Clarisse, L.: TES ammonia retrieval strategy and global observations of the spatial and seasonal variability of ammonia, Atmos. Chem. Phys., 11(20), 10743–10763, doi:10.5194/acp-11-10743-2011, 2011.

Singh, S. P., Satsangi, G. S., Khare, P., Lakhani, A., Maharaj Kumari, K. and Srivastava, S. S.: Multiphase measurement of atmospheric ammonia, Chemosph. - Glob. Chang. Sci., 3(1), 107–116, doi:https://doi.org/10.1016/S1465-9972(00)00029-5, 2001.

Sun, F., Cui, Y., Su, J., Shephard, M. W., Kharol, S. K., Zhang, Y., Shi, X., Zhang, J., Liu, H., Xiao, Q., Lu, X., Zeng, Z.-C., Griffis, T. J. and Hu, C.: Decadal changes in atmospheric ammonia and dry deposition across China inferred from space-ground measurements and model simulations, Atmos. Chem. Phys., 25(23), 17907–17932, doi:10.5194/acp-25-17907-2025, 2025.

Sun, K., Cady-Pereira, K., Miller, D. J., Tao, L., Zondlo, M. A., Nowak, J. B., Neuman, J. A., Mikoviny, T., Müller, M., Wisthaler, A., Scarino, A. J. and Hostetler, C. A.: Validation of TES ammonia observations at the single pixel scale in the San Joaquin Valley during DISCOVER-AQ, J. Geophys. Res. Atmos., 120(10), 5140–5154, doi:https://doi.org/10.1002/2014JD022846, 2015.

Sutton, M. A., Reis, S., Riddick, S. N., Dragosits, U., Nemitz, E., Theobald, M. R., Tang, Y. S., Braban, C. F., Vieno, M., Dore, A. J., Mitchell, R. F., Wanless, S., Daunt, F., Fowler, D., Blackall, T. D., Milford, C., Flechard, C. R., Loubet, B., Massad, R., Cellier, P., Personne, E., Coheur, P. F., Clarisse, L., Van Damme, M., Ngadi, Y., Clerbaux, C., Skjøth, C. A., Geels, C., Hertel, O., Wichink Kruit, R. J., Pinder, R. W., Bash, J. O., Walker, J. T., Simpson, D., Horváth, L., Misselbrook, T. H., Bleeker, A., Dentener, F. and de Vries, W.: Towards a climate-dependent paradigm of ammonia emission and deposition, Philos. Trans. R. Soc. Lond. B. Biol. Sci., 368(1621), 20130166, doi:10.1098/rstb.2013.0166, 2013.

Sutton, M. A., Asman, W. A. H., Ellermann, T., Van Jaarsveld, J. A., Acker, K., Aneja, V., Duyzer, J., Horvath, L., Paramonov, S., Mitosinkova, M., Tang, Y. S., Achermann, B., Gauger, T., Bartniki, J., Neftel, A. and Erisman, J. W.: Establishing the Link between Ammonia Emission Control and Measurements of Reduced Nitrogen Concentrations and Deposition, Environ. Monit. Assess., 82(2), 149–185, doi:10.1023/A:1021834132138, 2003.

Sutton, M. A., Tang, Y. S., Dragosits, U., Fournier, N., Dore, A. J., Smith, R. I., Weston, K. J. and Fowler, D.: A Spatial Analysis of Atmospheric Ammonia and Ammonium in the U.K., Sci. World J., 1(2), 268264, doi:https://doi.org/10.1100/tsw.2001.313, 2001.

Puchalski, M. A., Sather, M. E., Walker, J. T., Lehmann, C. M. B., Gay, D. A., Mathew, J. and Robarge, W. P.: Passive ammonia monitoring in the United States: Comparing three different sampling devices, J. Environ. Monit., 13(11), 3156–3167, doi:10.1039/C1EM10553A, 2011.

Tang, Y. S., Braban, C. F., Dragosits, U., Dore, A. J., Simmons, I., van Dijk, N., Poskitt, J., Dos Santos Pereira, G., Keenan, P. O., Conolly, C., Vincent, K., Smith, R. I., Heal, M. R. and Sutton, M. A.: Drivers for spatial, temporal and long-term trends

https://doi.org/10.5194/egusphere-2026-3909
Preprint. Discussion started: 24 July 2026

in atmospheric ammonia and ammonium in the UK, Atmos. Chem. Phys., 18(2), 705–733, doi:10.5194/acp-18-705-2018, 2018.

Tang, Y. S., Dragosits, U., van Dijk, N., Love, L., Simmons, I. and Sutton, M. A.: Assessment of Ammonia and Ammonium Trends and Relationship to Critical Levels in the UK National Ammonia Monitoring Network (NAMN) BT - Atmospheric Ammonia: Detecting emission changes and environmental impacts, edited by M. A. Sutton, S. Reis, and S. M. H. Baker, pp. 187–194, Springer Netherlands, Dordrecht., 2009.

Tang, Y., Cape, J., and Sutton, M. A.: Development and types of passive samplers for monitoring atmospheric NO2 and NH_3 concentrations, Sci. World J., 1, 513-529, doi: 10.1100/tsw.2001.82, 2001.

Tichý, O., Eckhardt, S., Balkanski, Y., Hauglustaine, D. and Evangeliou, N.: Decreasing trends of ammonia emissions over Europe seen from remote sensing and inverse modelling, Atmos. Chem. Phys., 23(24), 15235–15252, doi:10.5194/acp-23-15235-2023, 2023.

Twigg, M. M., Berkhout, A. J. C., Cowan, N., Crunaire, S., Dammers, E., Ebert, V., Gaudion, V., Haaima, M., Häni, C., John, L., Jones, M. R., Kamps, B., Kentisbeer, J., Kupper, T., Leeson, S. R., Leuenberger, D., Lüttschwager, N. O. B., Makkonen, U., Martin, N. A., Missler, D., Mounsor, D., Neftel, A., Nelson, C., Nemitz, E., Oudwater, R., Pascale, C., Petit, J.-E., Pogany, A., Redon, N., Sintermann, J., Stephens, A., Sutton, M. A., Tang, Y. S., Zijlmans, R., Braban, C. F. and Niederhauser, B.: Intercomparison of in situ measurements of ambient NH$_{3}$: instrument performance and application under field conditions, Atmos. Meas. Tech., 15(22), 6755–6787, doi:10.5194/amt-15-6755-2022, 2022.

Van Damme, M., Clarisse, L., Franco, B., Sutton, M. A., Erisman, J. W., Wichink Kruit, R., van Zanten, M., Whitburn, S., Hadji-Lazaro, J., Hurtmans, D., Clerbaux, C. and Coheur, P.-F.: Global, regional and national trends of atmospheric ammonia derived from a decadal (2008–2018) satellite record, Environ. Res. Lett., 16(5), 55017, doi:10.1088/1748-9326/abd5e0, 2021.

Van Damme, M., Clarisse, L., Whitburn, S., Hadji-Lazaro, J., Hurtmans, D., Clerbaux, C. and Coheur, P.-F.: Industrial and agricultural ammonia point sources exposed, Nature, 564(7734), 99–103, doi:10.1038/s41586-018-0747-1, 2018.

Viatte, C., Guendouz, N., Dufaux, C., Hensen, A., Swart, D., Van Damme, M., Clarisse, L., Coheur, P. and Clerbaux, C.: Measurement report: Ammonia in Paris derived from ground-based open-path and satellite observations, EGUsphere, 2023, 1–23, doi:10.5194/egusphere-2023-963, 2023.

Volten, H., Bergwerff, J. B., Haaima, M., Lolkema, D. E., Berkhout, A. J. C., van der Hoff, G. R., Potma, C. J. M., Wichink Kruit, R. J., van Pul, W. A. J. and Swart, D. P. J.: Two instruments based on differential optical absorption spectroscopy (DOAS) to measure accurate ammonia concentrations in the atmosphere, Atmos. Meas. Tech., 5(2), 413–427, doi:10.5194/amt-5-413-2012, 2012.

von Bobrutzki, K., Braban, C. F., Famulari, D., Jones, S. K., Blackall, T., Smith, T. E. L., Blom, M., Coe, H., Gallagher, M., Ghalaieny, M., McGillen, M. R., Percival, C. J., Whitehead, J. D., Ellis, R., Murphy, J., Mohacsi, A., Pogany, A., Junninen, H., Rantanen, S., Sutton, M. A. and Nemitz, E.: Field inter-comparison of eleven atmospheric ammonia measurement techniques, Atmos. Meas. Tech., 3(1), 91–112, doi:10.5194/amt-3-91-2010, 2010.

https://doi.org/10.5194/egusphere-2026-3909
Preprint. Discussion started: 24 July 2026

Wang, R., Pan, D., Guo, X., Sun, K., Clarisse, L., Van Damme, M., Coheur, P.-F., Clerbaux, C., Puchalski, M. and Zondlo, M. A.: Bridging the spatial gaps of the Ammonia Monitoring Network using satellite ammonia measurements, Atmos. Chem. Phys., 23(20), 13217–13234, doi:10.5194/acp-23-13217-2023, 2023.

Wang, W., Liu, C., Clarisse, L., Van Damme, M., Coheur, P.-F., Xie, Y., Shan, C., Hu, Q., Sun, Y. and Jones, N.: Ground-based measurements of atmospheric NH_3 by Fourier transform infrared spectrometry at Hefei and comparisons with IASI data, Atmos. Environ., 287, 119256, doi:https://doi.org/10.1016/j.atmosenv.2022.119256, 2022.

Warner, J. X., Dickerson, R. R., Wei, Z., Strow, L. L., Wang, Y. and Liang, Q.: Increased atmospheric ammonia over the world's major agricultural areas detected from space, Geophys. Res. Lett., 44(6), 2875–2884, doi:https://doi.org/10.1002/2016GL072305, 2017.

Xie, Y., Wang, W., Chen, Y., Qian, Z., Chen, J., Tong, J., Li, L., Yue, Y., Chen, K., Chu, Z. and Hu, X.: NH_3 Emissions and Lifetime Estimated by Satellite Observations with Differential Evolution Algorithm, Atmosphere (Basel)., 15(3), doi:10.3390/atmos15030251, 2024.

Yamanouchi, S., Viatte, C., Strong, K., Lutsch, E., Jones, D. B. A., Clerbaux, C., Van Damme, M., Clarisse, L. and Coheur, P.-F.: Multiscale observations of NH_3 around Toronto, Canada, Atmos. Meas. Tech., 14(2), doi:10.5194/amt-14-905-2021, 2021.

van Zanten, M. C., Wichink Kruit, R. J., Hoogerbrugge, R., Van der Swaluw, E. and van Pul, W. A. J.: Trends in ammonia measurements in the Netherlands over the period 1993–2014, Atmos. Environ., 148, 352–360, doi:https://doi.org/10.1016/j.atmosenv.2016.11.007, 2017.

Zhu, L., Henze, D. K., Bash, J. O., Cady-Pereira, K. E., Shephard, M. W., Luo, M. and Capps, S. L.: Sources and Impacts of Atmospheric NH_3: Current Understanding and Frontiers for Modeling, Measurements, and Remote Sensing in North America, Curr. Pollut. Reports, 1(2), 95–116, doi:10.1007/s40726-015-0010-4, 2015.